

Chapter 3

THE INSTRUMENT

3.1 Overview of the instrument

Basically, the instrument designed was a spectrograph to obtain coronal spectra of the solar corona during the total solar eclipse of August 11, 1999.

However this design incorporated a new feature in the way the light was collected and fed to the spectrograph in obtaining spectra. The exception from the usual slit-based spectrograph was that light was collected at the focal plane of the telescope via fiber optics. The fiber optic tips at the focal plane of the telescope were positioned at various latitudes and radii on the image of the sun formed on the focal plane of the telescope during the solar eclipse. This method served two very important purposes.

1. This way the instrument was able to obtain **simultaneous coronal spectra from different latitudes and radii on the solar corona.**

2. Also as a complimentary the telescope was spared the task of carrying the weight of the spectrograph. This was because they were detached systems connected via fiber optic cables.

In essence the instrument was composed of three vital components.

1. The telescope imaged the sun during the eclipse on the focal plane of the telescope.
2. The fiber optic tips, positioned at various latitudes and radii on the sun's image on the focal plane of the telescope, carried the coronal light to the spectrograph.
3. The spectrograph produced simultaneous spectra from the light received by the individual fibers.

The telescope used in this experiment was a Schmidt-Cassegrain telescope with a primary mirror diameter of 12-inches and a focal ratio of 10.0. A focal reducer was attached to reduce the focal ratio to 6.3. Schmidt-Cassegrain telescopes by design are free from coma, spherical aberration and astigmatism. The telescope also contained auto-tracking capability. Figure (3.1) is a picture of the telescope used in this experiment and produced by the Meade Corporation. Figure (3.2) is a picture of the focal reducer attached to the back end of the telescope that increased the field of view by 56.0 % at the expense of lowering the magnifying power by 36.0 %.

At the focal plane of the telescope was a glass plate embedded with twenty-one fiber optic tips with ten each spread in equal angles in a circular loop corresponding to 1.1 and 1.5 solar radii on the sun's image and one at the center of the frame. The one in the center of the frame was used to record the background signal using the lunar shadow during the eclipse. Another four fibers were attached to a mercury calibration lamp.



Figure (3.1). Meade 12-inch, F/10.0 Schmidt-Cassegrain telescope with auto tracking capabilities.

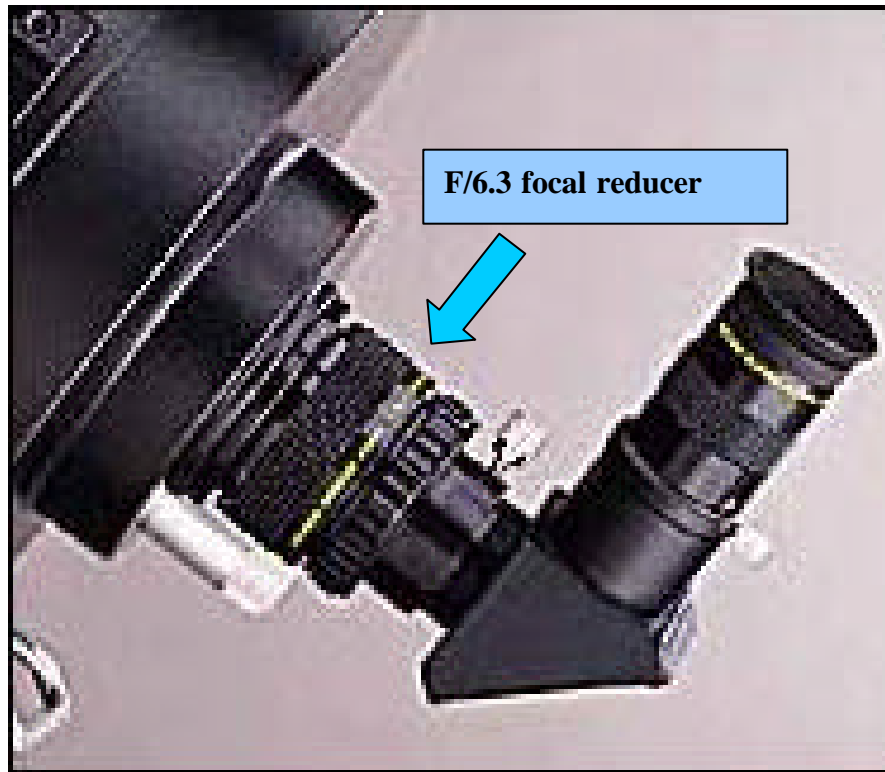


Figure (3.2). F/6.3 focal reducer reduces the focal length by a factor of 0.63. The device shown in figure (3.4) was placed at the focal plane behind the F/6.3 focal reducer.

Figure (3.3) shows a schematic of the glass plate, as it would appear when the sun is in focus. Figure (3.4) shows the picture of the fiber optic tips embedded on the glass plate. The front end of the glass plate, where the fiber ends were exposed to the coronal light, was roughened with the back end smoothed. This allowed for the focusing of the sun prior to the eclipse on the front end of the glass while observing the image going in and out of focus from the back end. The fiber in the center was to record the background signal during the eclipse.

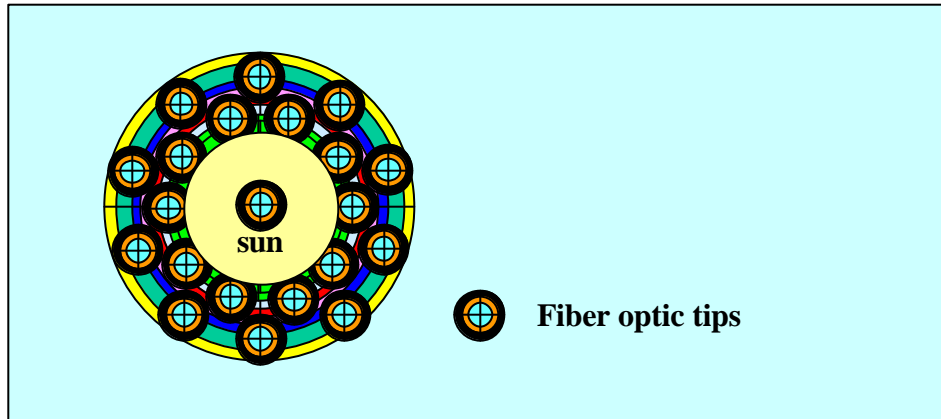


Figure (3.3) A drawing depicting the location of the fiber tips on the image plane of the telescope. The inner and outer rings are at 1.1 and 1.5 solar radii, respectively. During the eclipse the lunar shadow replaces the sun.

In figure (3.4) is the glass plate imbedded with twenty-one fibers that was placed at the focal plane of the telescope. The coronal light entering the fibers, which were located at the focal plane of the telescope and shown in figure (3.4), were all vertically aligned at the other end. The other end substitutes the position of the slit in a slit-based spectrograph. This slit, made up of multiple fibers at regular spacing between neighbors, was placed at the prime focus of the collimating lens of the spectrograph. In figures (3.5) and (3.6) are images of the spectrograph.

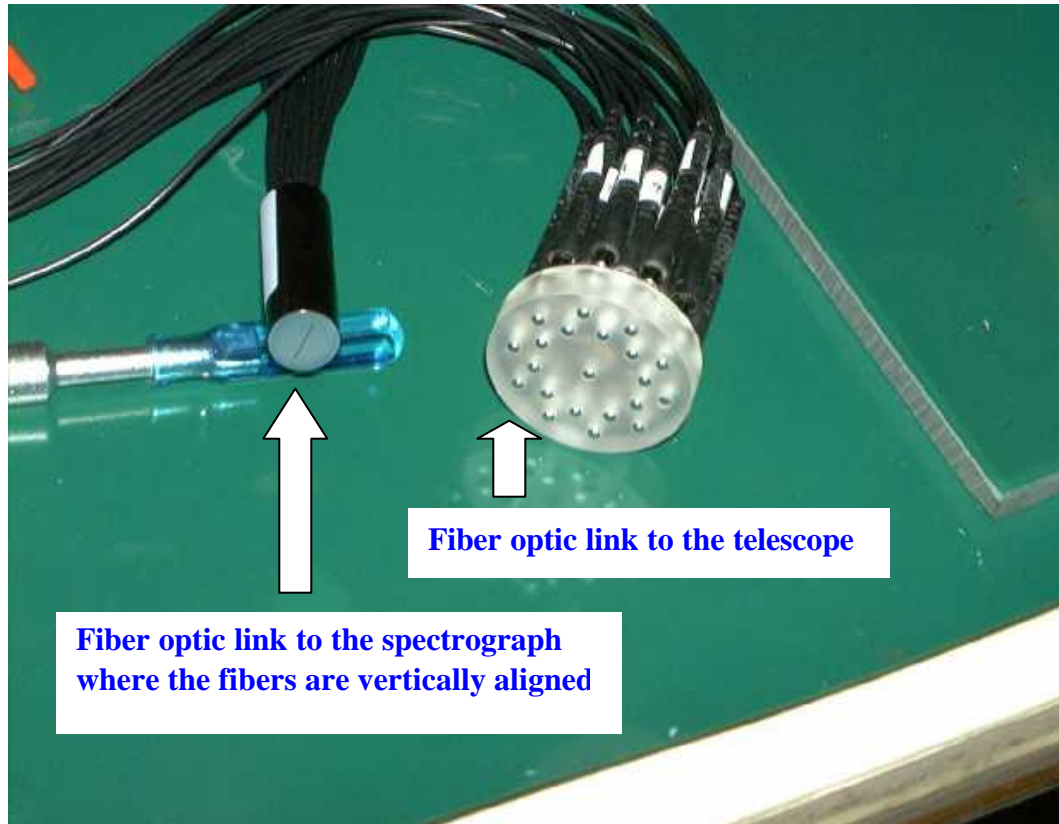


Figure (3.4). The glass plate imbedded with twenty-one fibers. The inner and the outer circles are located at 1.1 and 1.5 solar radii, respectively, on the image plane of the sun. The fiber at the center was to record the background signal during the eclipse.

From figure (3.5) it is apparent that, apart from the capability of this setup to simultaneously produce spectra, this methodology also allowed for the telescope and the spectrograph to be two independent units connected via light fiber optic cables. This is not possible in a slit-based spectrograph. In such a case the spectrograph needs to be attached to the back end of the telescope with the slit at the focal points of both the telescope and the collimating lens of the spectrograph. The purpose of the collimating lens is to transmit collimated light to the diffraction grating for dispersion.

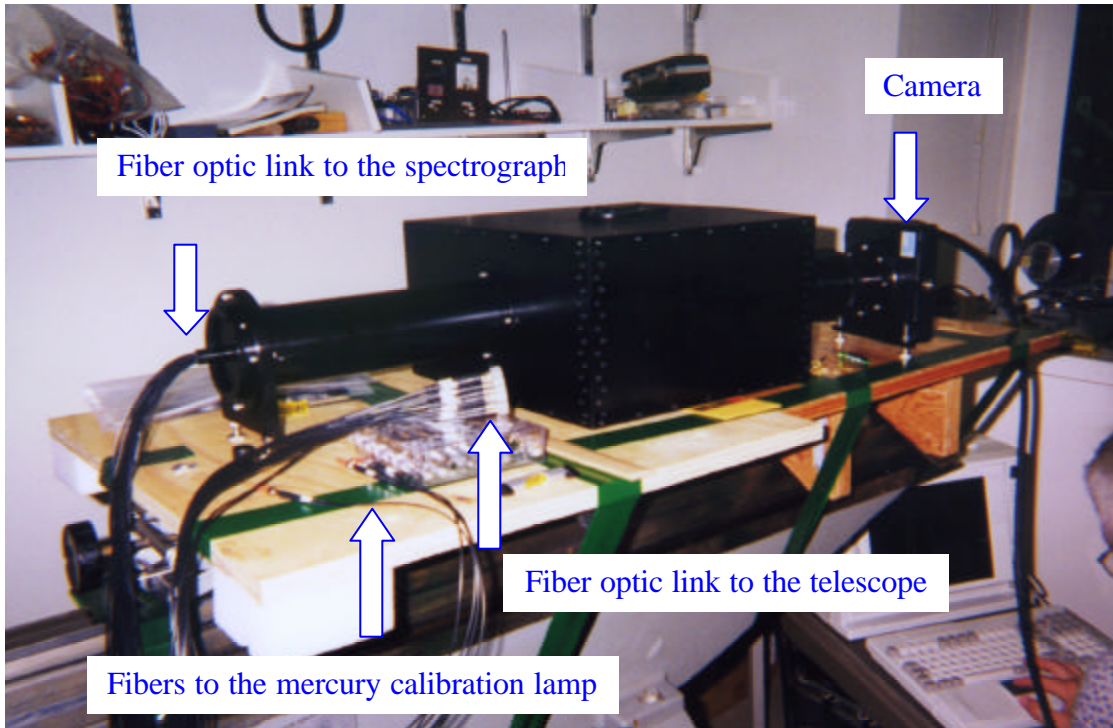


Figure (3.5). This is a picture of the spectrograph. The coronal light was fed into the spectrograph by twenty-one fibers that were vertically arranged at a regular spacing. Its location in the spectrograph was at the focal point of the collimating lens.

Figure (3.6) shows the inside of the spectrograph between the grating and the camera lens that focuses the dispersed light to the camera in the backend. The spectrograph body contained many features that made it light tight from stray light that could have found its way into the spectrograph. Also the setscrews ensured that the many parts of the spectrograph fitted in place during assembly as a single unit.

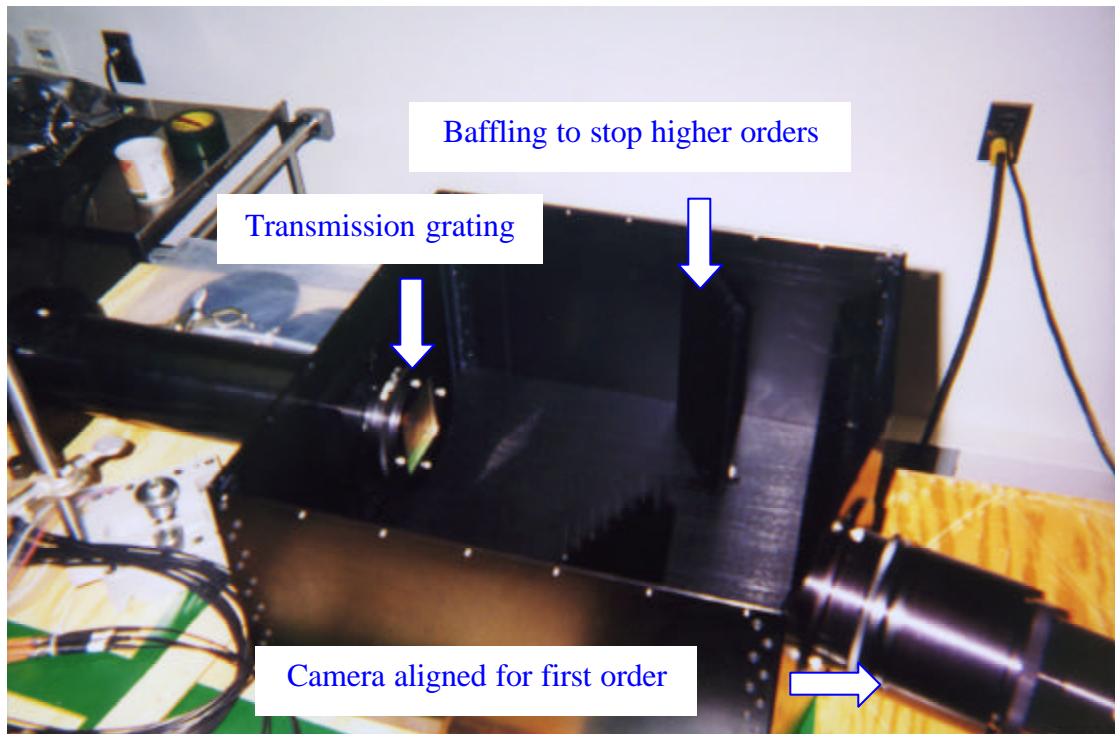


Figure (3.6). This is a picture of the inside of the spectrograph between the grating and the camera lens. Baffling were used to prevent all orders but the first order from entering into the camera lens.

In figure (3.7) is a picture of the CCD camera that was used in this experiment to record the light dispersed in the first order in the wavelength region of 3500.0 to 4500.0 angstroms. A thermoelectric cooler cooled the CCD device. Baffling were placed to restrict only the dispersed light in the first order from entering the camera. All the other orders were subjected to multiple reflections within the saw-tooth shaped grooves in the baffles for absorption by the black-coated baffling material.

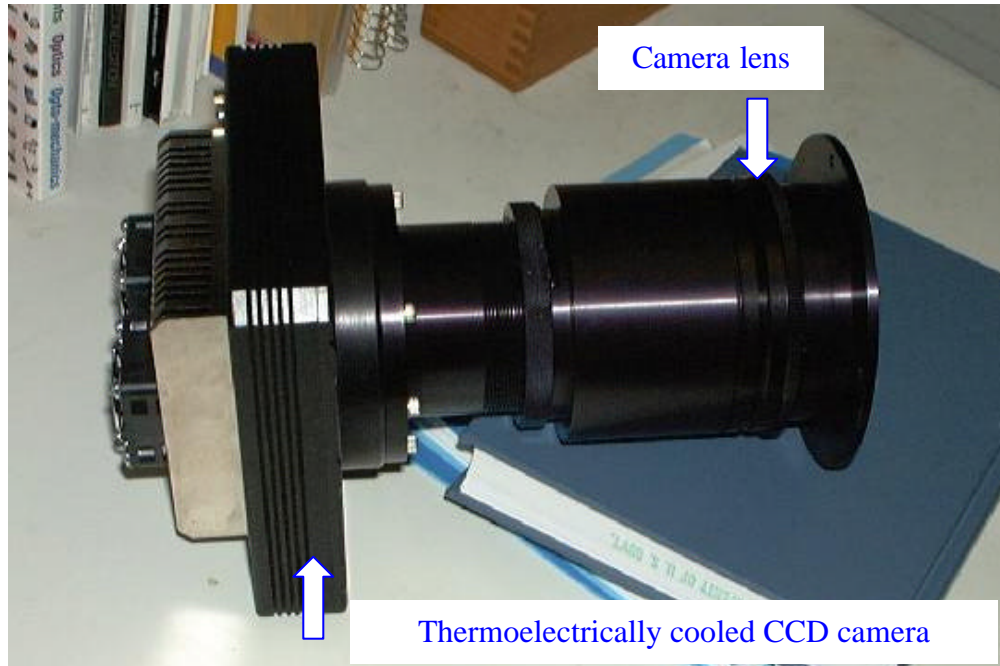


Figure (3.7). This is a picture of the thermoelectrically cooled CCD camera used in the experiment. The front end housed the camera lens that focused the dispersed light from the grating on to the camera.

As a general overview of the instrument the following could be said. The telescope imaged the eclipsed sun on to a glass plate containing twenty-one fibers, which was located at the focal plane of the telescope. The fibers picked up the light from various locations on the sun's corona and the moon's center. This light was fed to a spectrograph via the fiber optic cables. Then the grating simultaneously dispersed lights from all the fibers. The camera located at the backend of the spectrograph recorded the dispersed light in the first order in the wavelength region of 3500.0 to 4500.0 angstroms. In view of this instruments ability to record simultaneous spectra it was deemed appropriate to name this system the **Multi Aperture Coronal Spectrometer** with the acronym (**MACS**).

3.2 Description of the optical elements in detail

In the following subsections all the optical elements of MACS will be discussed in details.

3.2.1 The telescope

The telescope used in MACS was a 12-inch F/10.0 Schmidt-Cassegrain manufactured by the Meade Corporation. The f-number was reduced to F/6.3 using a focal reducer in order to increase the plate scale. The LX200 model used in MACS also featured auto tracking and a super wedge for polar alignment. By design the Schmidt-Cassegrain type telescopes eliminate image distortion due to coma, spherical aberration and astigmatism, which are explained below. These optical systems are also called *anastigmats* and consist of at least three optical elements. A Schmidt-Cassegrain telescope consists of a concave and convex mirrors as the primary and the secondary, respectively, and a thin aspheric corrector plate in the front.

Spherical aberration: Parallel rays are not brought to a focus at a point, but along a line. Therefore off-axis rays are brought to a focus closer to the lens than are on-axis rays.

Coma: Off-axis rays do not quite converge at the focal plane, thus rendering off-axis points with tails, reminiscent of comets, hence the name.

Astigmatism: Rays of different orientations having different focal lengths resulting in the distortion of the image. Rays of light from horizontal and vertical lines in a plane on the object are not focused to the same plane on the edges of the image. Off-axis points are blurred in their radial or tangential direction, and focusing can reduce one at the expense of the other.

The plate scale (**P**) of the telescope is defined as the spatial area seen in the sky, which is measured in arcseconds, corresponding to the spatial scale in the focal plane of the telescope, which is measured in micrometers and shown in figure (3.8).

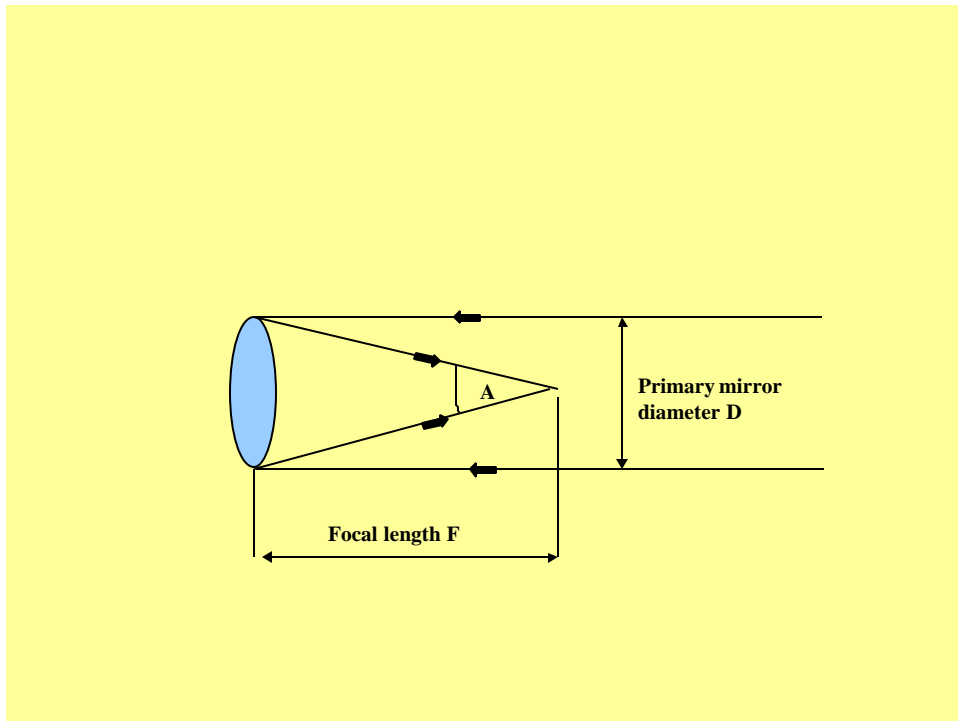


Figure (3.8). Schematic drawing on the image formation by the primary mirror of the telescope.

From figure (3.8) the expression for angle **A** is given by equation (3.1).

$$\mathbf{Tan(A) = \frac{D}{F}} \quad (3.1)$$

Since (**A**) is a small angle, expressing (**A**) in radians, where (**Tan (A) ≈ A**), and then converting radians into arcseconds, where (**1 radian = 206265**) arcseconds, gives the following expression for (**A**), as shown in equation (3.2).

$$\mathbf{A = \frac{206265 \cdot D}{F}} \quad (3.2)$$

From the definition of the plate scale (**P**) it could be written as shown in equation (3.3).

$$\mathbf{P = \frac{A}{D}} \quad (3.3)$$

$$= \frac{206265 \cdot D / F}{D}$$

$$= \frac{206265}{D \cdot \frac{F}{D}}$$

$$= \frac{206265}{D \cdot F / \#} \text{ arcseconds /mm}$$

Substituting for the diameter of the primary **D** in **mm** (12-inch = 12×2.54 cm = $12 \times 2.54 \times 10^4$ **mm**) and the f-number of the telescope ($F/\# = 6.3$) in equation (3.3) gives the following value for the plate scale (**P**) as shown in equation (3.4).

$$\boxed{\mathbf{P = 0.107 \text{ arcseconds /mm}}} \quad (3.4)$$

3.2.2 The fibers

The fibers linking the focal plane of the telescope and the spectrograph were twenty-one fibers with four more connected to a mercury calibration lamp. Each of these fibers was 1.0 m in length with a core diameter of 200.0 **mm**. Figure (3.9) shows the transmission efficiency of the fibers, marked as UV/VIS, for the region of wavelength interest which was from 3500.0 – 4500.0 angstroms. These fibers were purchased from Oriel Corporation.

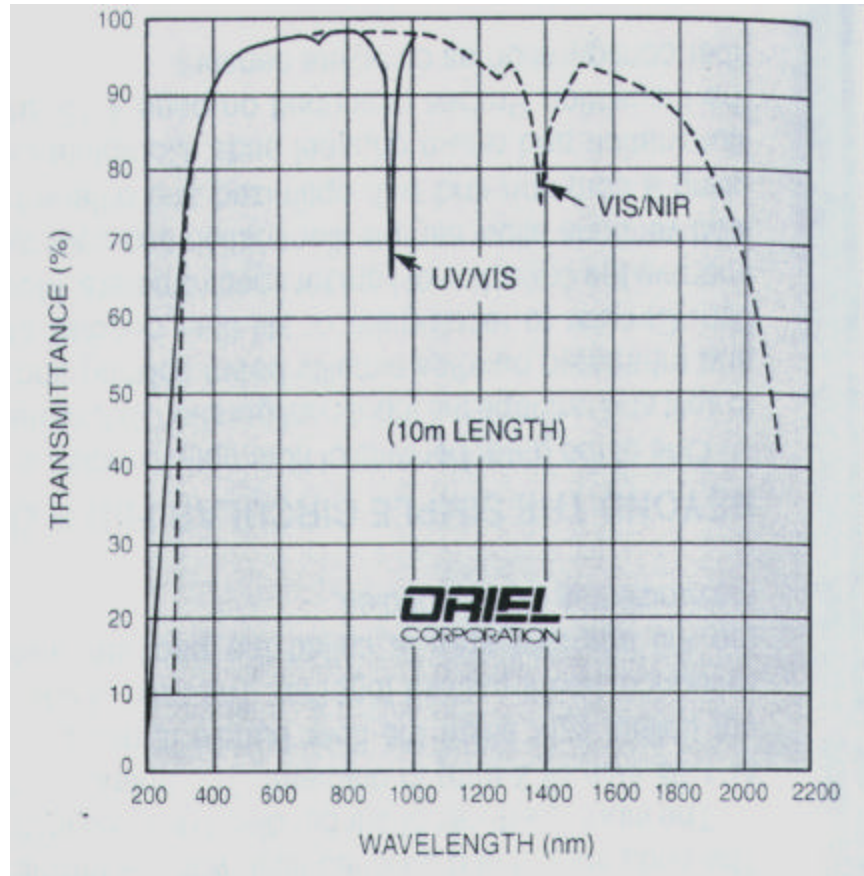


Figure (3.9) Transmission efficiency of the fibers used in MACS and marked as UV/VIS. The region of wavelength interest in MACS was from 3500.0 –4500.0 angstroms.

All optical fibers transmit light signals by total internal reflection. That is, if a ray of light in a medium of refractive index n_1 strikes the interface with another medium of refractive index n_2 ($n_2 < n_1$) at an angle q , and if q is greater than q_c , the ray is totally reflected back in to the first medium where q_c is given by equation (3.5).

$$q_c = \sin^{-1}\left(\frac{n_2}{n_1}\right) \quad (3.5)$$

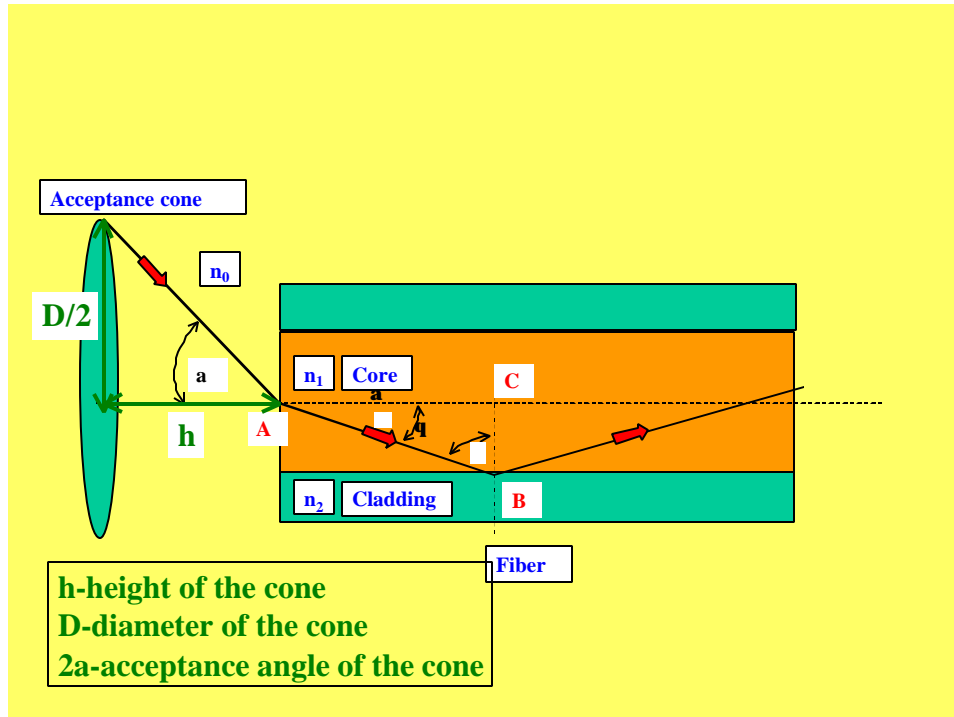


Figure (3.10). Schematic diagram depicting the light ray path at the focal plane of the telescope into a fiber optic cable.

Figure (3.10) is a schematic drawing depicting the light ray path at the focal plane of the telescope into a fiber optic cable. At point (A) applying the Snell's law gives the relationship between angles (a and a) and refractive indices (n_0 and n_1) by equation (3.6).

$$\sin(a) \cdot n_0 = \sin(a) \cdot n_1 \tag{3.6}$$

Now from triangle ABC the expression for angle q is given by equation (3.7).

$$\begin{aligned}
 q &= 90 - a \\
 \sin(q) &= \cos(a) \\
 &= \sqrt{1 - \sin^2(a)}
 \end{aligned}$$

$$\tag{3.7}$$

At the critical angle ($q = q_c$) using equations (3.5), (3.6) and (3.7) the expression for the acceptance angle (\mathbf{a}) in terms of the refractive indices is given by equation (3.8).

$$\sin(\mathbf{a}) = \frac{\sqrt{n_1^2 - n_2^2}}{n_0} \text{ and } n_0 \sim 1 \quad (3.8)$$

The sine of the acceptance angle (\mathbf{a}) is defined as the numerical aperture (\mathbf{NA}). Also from figure (3.10), the expression for $\sin(\mathbf{a})$ is given by equation (3.9).

$$\boxed{\begin{aligned} \sin(\mathbf{a}) &= \frac{D/2}{h} \\ &= \frac{1}{2 \frac{h}{D}} \\ &= \frac{1}{2(\mathbf{F/\#})} \end{aligned}} \quad (3.9)$$

The fibers used in MACS have a high purity UV grade silica core and silica glass cladding with a numerical aperture of 0.27. This corresponds to an acceptance cone angle ($2\mathbf{a}$) of 31.0 degrees and an f-number ($\mathbf{F/\#}$) of 1.9.

All the light rays entering the fiber within the acceptance cone is totally reflected at the core-cladding boundary inside the fiber and the signal is transmitted to the other end. That is, all light rays within the acceptance cone entering the fiber at an angle less than the acceptance angle (\mathbf{a}) strike the core-cladding interface at an angle greater than the critical angle q_c . This fulfils the requirement for total internal reflection at the core-cladding boundary.

The f-number of the telescope used in MACS was F/6.3, which corresponds to an acceptance cone of 9.1 degrees. However this value was much less than the acceptance cone of 31.0 degrees for the fibers. Therefore all the light that was focused onto each of the fibers at the focal plane of the telescope was expected to be transmitted.

The emergent cone from the other end of the fiber is dependent upon the input illumination, the fiber properties and the layout of the fiber bundle. For long fibers, the fiber properties dominate, while for short fibers (< 1.0 to 2.0 m) the input conditions dominate. Since the fibers in MACS were 1.0 m in length the emergent cone was expected to closely resemble the input conditions.

3.2.3 The lenses

The spectrograph contained two lenses of diameter 8.0 cm each with f-numbers F/3.9 and F/2.0. The former functioned as a collimator to collimate the light given out by the fibers. This enabled the grating to receive collimated light for dispersion. The latter acted as a focusing lens to focus the dispersed light on to the camera. Spindler & Hoyer manufactured these achromatic lenses. An anti UV-reflective coating was applied on the lens surfaces in order to enhance the transmission below 4000.0 angstrom. Figure (3.11) shows the reflection properties for the anti UV-reflective coating. Very low reflection ensures greater transmission. This was achieved with ARB2 UV chemical coating.

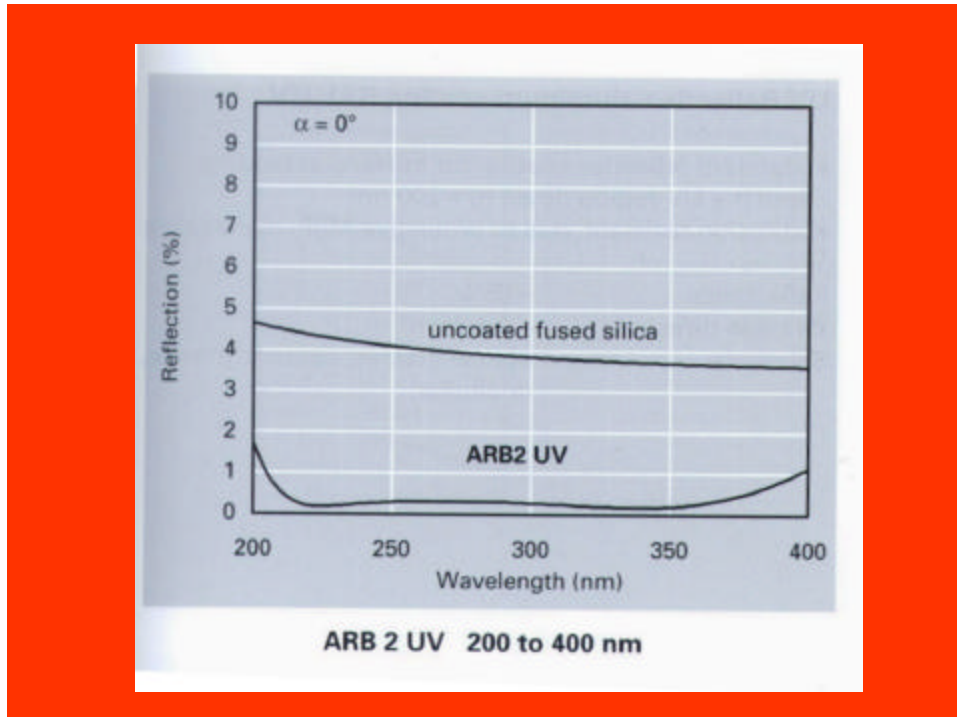
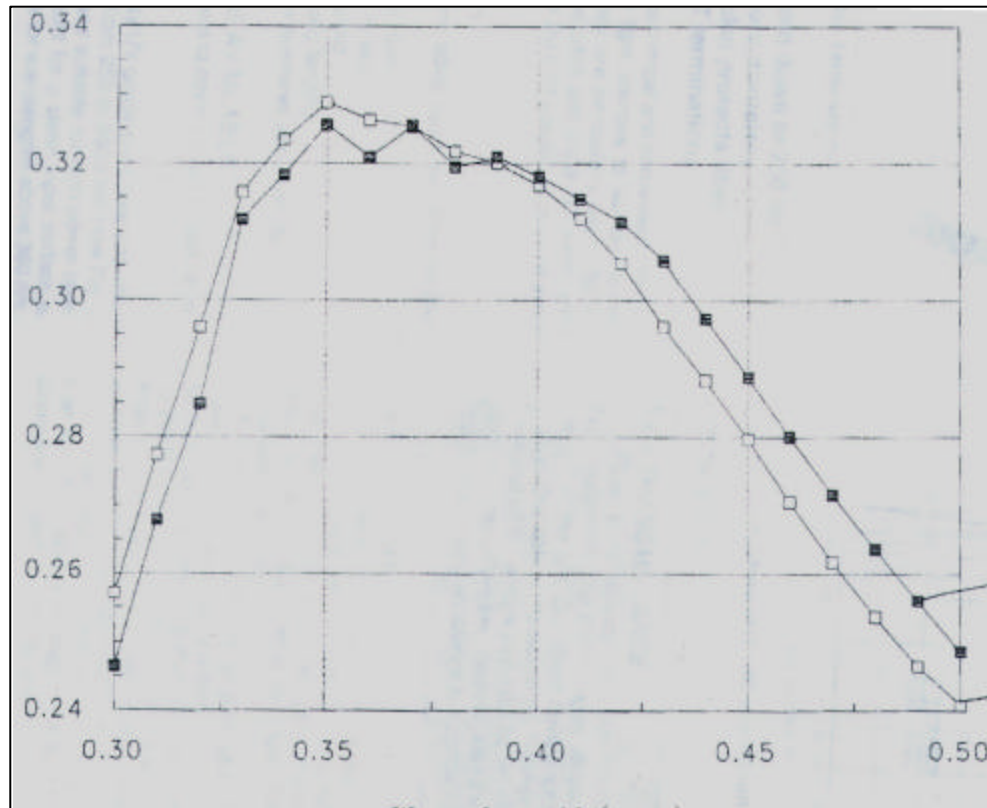


Figure (3.11). Reflection properties for the anti UV-reflective coating on the collimating and the camera lenses used in the spectrograph.

3.2.4 The grating

The dispersing element used in MACS was a square transmission grating of dimensions $6.0 \times 6.0 \text{ cm}^2$ with 6000.0 lines per cm and anti UV-reflective coating for enhanced transmission. Figure (3.12) shows the transmission properties for the anti UV-reflective coating. This grating was manufactured by American Holographic.

Efficiency



Wavelength $\times 10^4$ Angstrom

Figure (3.12). Transmission properties at normal incidence for the anti UV-reflection coating on the transmission grating. Here the back surface reflection is not considered. The substrate material is fused silica. The black squares pertain to the grating used in MACS.

3.2.5 The camera

The camera used in MACS was a CCD camera with a back thinned SITE 512.0×512.0, 24.0mm square chip and controlled with *PMIS* camera-control software. *PMIS* contains a powerful command interpreter designed for automating repetitive or complex actions. The camera can also be thermoelectrically cooled from 50.0⁰ – 60.0⁰ C below ambient and was manufactured by Apogee Instruments, Inc. Figure (3.13) is a plot of the quantum efficiency (QE) curve for the for the CCD chip in the camera.

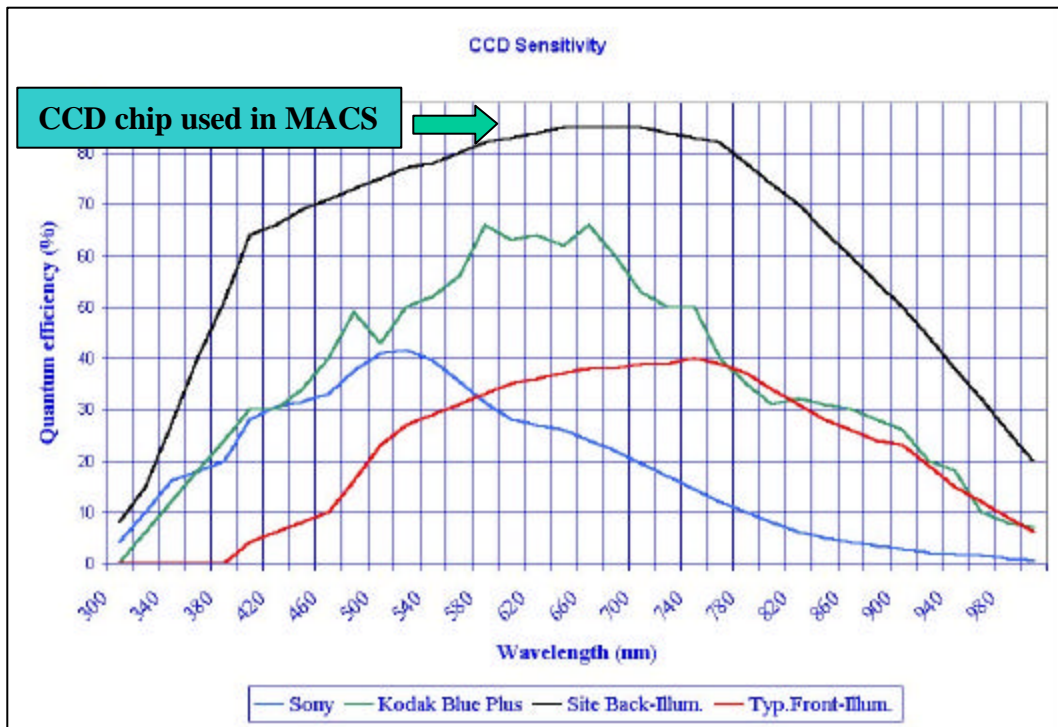


Figure (3.13). Quantum efficiency (QE) curve for the back thinned SITE 512.0×512.0, 24.0mm square chip used in MACS. This chip also featured a full well depth in excess of 300,000.0 electrons, a dynamic range of ~ 90.0 dB and a readout time of ~ 5.0 seconds with an ISA card.

3.3 Analytical expressions for the integration time, the spectral resolution and the spatial resolution

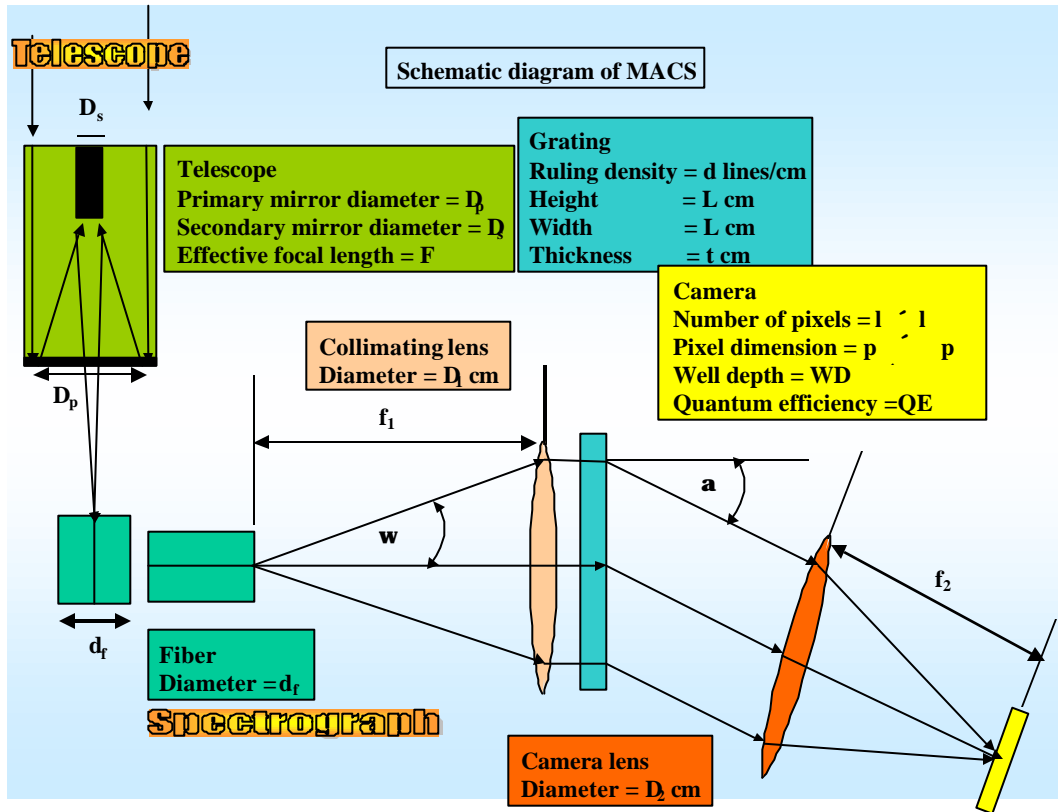


Figure (3.14). Schematic diagrams of the optical components that make up MACS and the parameters that determine the spatial and the spectral resolutions.

Figure (3.14) is a schematic diagram of the optical components that contributed to the operation of MACS and the physical parameters of the different components that determined the spectral and the spatial resolutions. In MACS the fibers substituted for a slit in a slit based spectrograph.

Consider a single fiber of diameter (d_f) and approximate the circular end of the fiber to a square of side (d_f). The projected fiber width (w) and height (h) on the camera focal plane are, respectively, given by equation (3.10) and equation (3.11).

$$w = d_f \frac{2 \cos(b)}{1 + \cos(a)} \quad (3.10)$$

$$h = d_f \frac{2}{1 + \cos(a)} \quad (3.11)$$

In equation (3.10) (b) is the angle of incidence on the grating and is zero for normal incidence, which is the case for MACS. The direction of the dispersion is along (w).

For normal incidence the grating equation is given by equation (3.12).

$$d \sin(a) = m\lambda \quad (3.12)$$

In equation (3.12) (d) is the ruling density, (a) the diffraction angle, (m) the diffraction order and (λ) the wavelength.

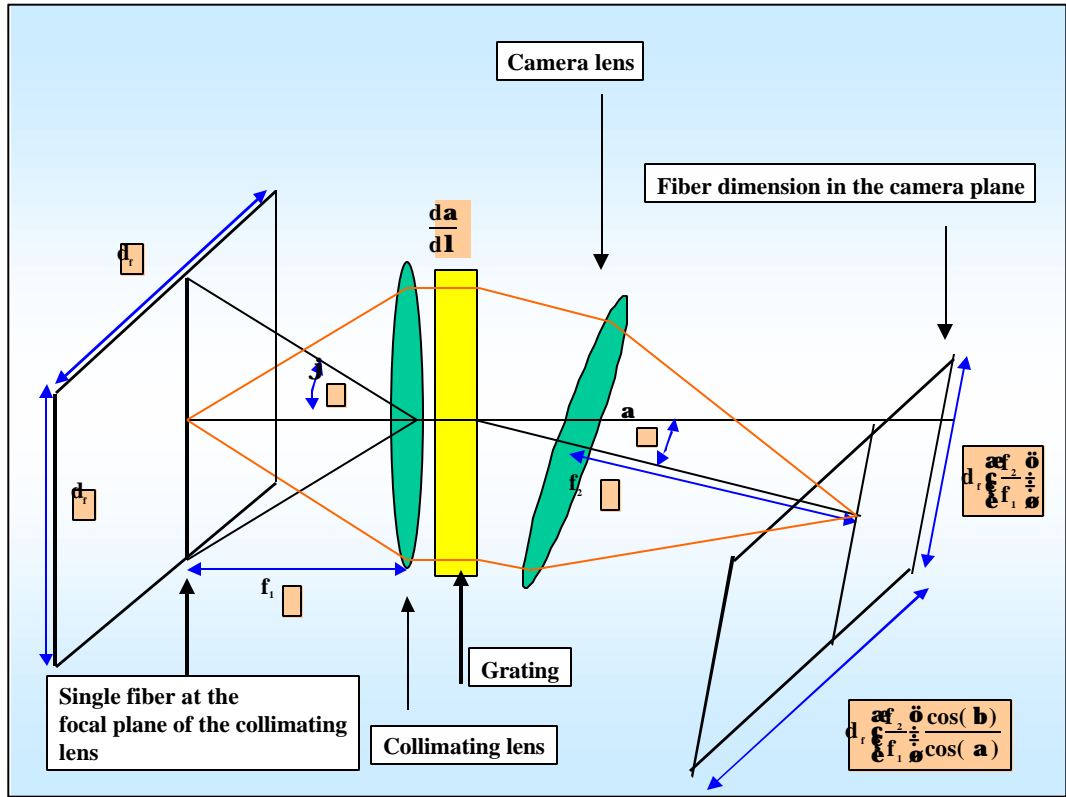


Figure (3.15). Schematic diagram showing the projected width and height of a single fiber on the camera plane.

Figure (3.15) is a schematic diagram showing the projected width and height of a single fiber on the camera plane.

For collimated light incident on the grating the angular dispersion is given by $(\frac{da}{dl})$, with the dispersion parallel to the rulings on the grating. Then the linear dispersion is given by $(f_2 \cdot (\frac{da}{dl}))$ where (f_2) is the focal length of the camera lens.

Using equation (3.12) the angular dispersion (**AD**) and the linear dispersion (**LD**) are given, respectively, by equation (3.13) and equation (3.14).

$$\begin{aligned} \mathbf{AD} &= \frac{da}{dl} \\ &= \frac{m}{d \cos(a)} \end{aligned} \quad (3.13)$$

$$\begin{aligned} \mathbf{LD} &= \frac{dl}{da} \\ &= f_2 \frac{da}{dl} \\ &= \frac{f_2 m}{d \cos(a)} \end{aligned} \quad (3.14)$$

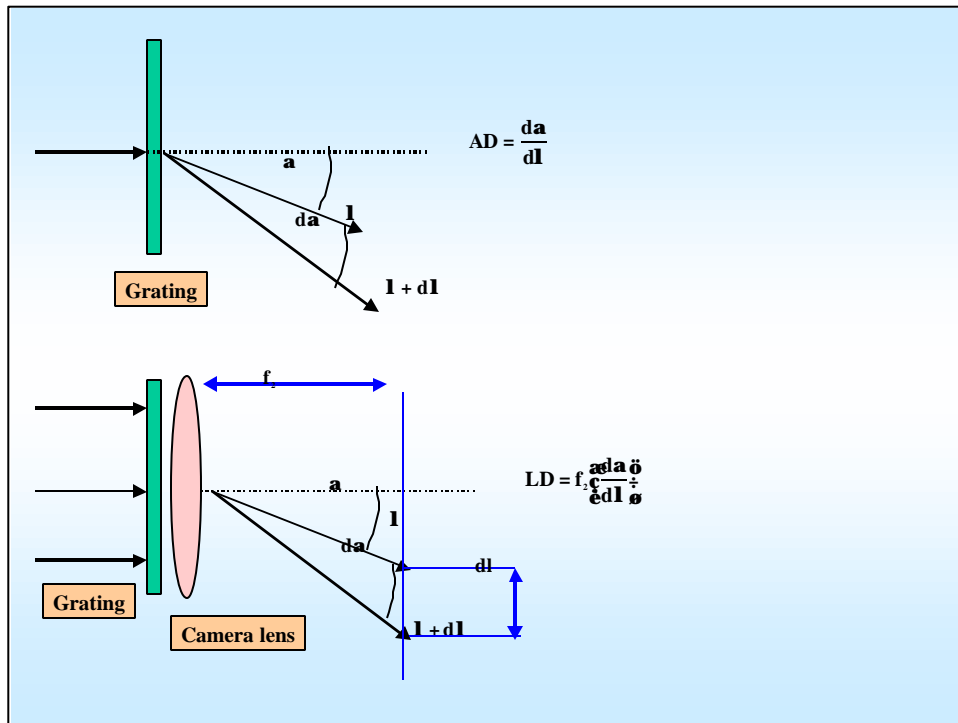


Figure (3.16). Schematic diagram of the dispersing element showing the angular and the linear dispersions.

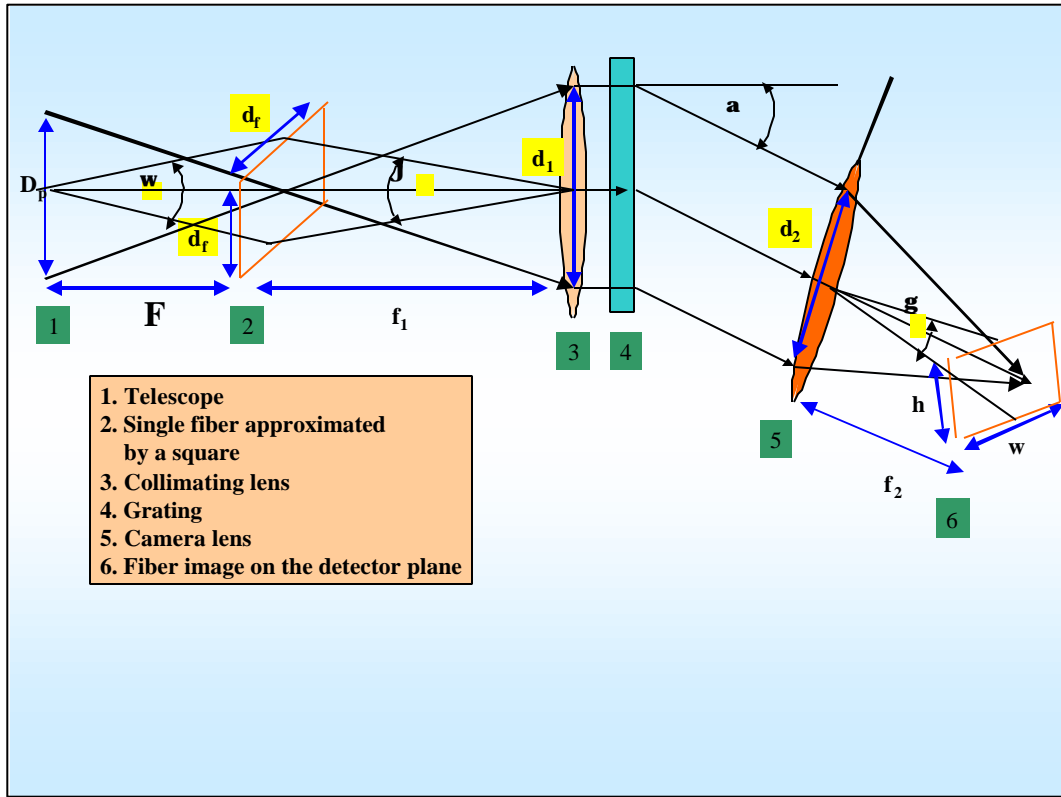


Figure (3.17). Schematic layout of the slit spectrometer. In this diagram collimated light is incident on the grating.

From figure (3.17) the height and width of the entrance slit (single fiber) subtend angles w and j on the sky and the collimating lens, respectively, and are given by equation (3.15) and equation (3.16).

$$w = \frac{D_p}{F} \tag{3.15}$$

$$j = \frac{d_f}{f_1} \tag{3.16}$$

If for the CCD detector the pixel width is (p) then it needs to be decided on how many pixels are to be allowed to match the image width (w). The usual convention is to consider a proper match to be one where two pixels cover the width (w). However in situations constrained by, time, amount of light expected from the object to be studied, transmission efficiency of the optics and resources available in obtaining the desired optical components, the decision rests on the compromise between resolution and allowing for sufficient transmission of light to the detector.

In the absence of such constraints, say (n) number of pixels are to be matched to the image width (w), then from equations (3.10), (3.11) and (3.15) the expression for the pixel width (w) is given by equation (3.17).

$$\begin{aligned}
 np &= w \\
 &= d_f \frac{f_2 \cos(b)}{f_1 \cos(a)} \\
 &= w F \frac{f_2 \cos(b)}{f_1 \cos(a)} \\
 &= w \frac{f_1}{D_p} \frac{f_2 \cos(b)}{f_1 \cos(a)} \\
 &= w D_p \frac{f_2 \cos(b)}{d_1 \cos(a)}
 \end{aligned}
 \tag{3.17}$$

In equation (3.17) the relationship ($f_1/d_1 = F/D_p$) is used together with the physical parameter for the beamwidth (d_1) at the collimating lens, as shown in figure (3.17). Here it is assumed that the grating diameter is at least (d_1).

Consider the spectrometer slit of width (d_f) illuminated with light of wavelengths (λ) and ($\lambda + d\lambda$). The slit image in each of these wavelengths will have a width (w) on the detector. From equation (3.14) the separation between the centers of these two images is given by equation (3.18).

$$d\lambda = \frac{f_2 m}{d \cos(a)} d\lambda \quad (3.18)$$

Now defining **spectral purity** ($d\lambda$) as the wavelength difference for which ($D\lambda = w$), ensuring the images are just resolved. Substituting this condition in equation (3.18) and also using equation (3.10) the spectral purity is given by equation (3.19).

$$d\lambda = \frac{w}{d \cos(a)} \frac{d \cos(a)}{f_2 m} = \frac{d_f d \cos(b)}{m f_1} \quad (3.19)$$

where ($b = 0$) for collimated light incident on the grating. However it needs to be noted that the expression for the spectral purity given by equation (3.19) cannot be smaller than the spectral purity limit ($d\lambda_0$) set by diffraction. The resolving power (R) of a grating is the ratio between the smallest change of wavelength that the grating can resolve and the wavelength at which it is operating. The resolving power is given by equation (3.20).

$$R = \frac{\lambda}{d\lambda} \quad (3.20)$$

From figure (3.18) the path difference (**DO**) between contributions from the center and the edge of the grating is given by equation (3.21).

$$\mathbf{DO} = \frac{L\zeta}{2} \sin(\mathbf{d a}) \quad (3.21)$$

Then the associated phase difference (x) is given by equation (3.22).

$$\begin{aligned} x &= \frac{2p}{l} \cdot \mathbf{DO} \\ &= \frac{2p}{l} \cdot \frac{L\zeta}{2} \sin(\mathbf{d a}) \\ &= \frac{2p}{l} \cdot \frac{L\zeta_0}{2f_2} \end{aligned} \quad (3.22)$$

The intensity distribution (I_z) at the focal plane, due to diffraction, is given by equation (3.23).

$$I_z = I_0 \frac{\sin^2(x)}{x^2} \quad (3.23)$$

The first minimum of equation (3.23) is for (x) given by equation (3.24).

$$\begin{aligned} x &= \frac{2p}{l} \cdot \frac{L\zeta_0}{2f_2} \\ &= p \end{aligned} \quad (3.24)$$

From equation (3.14) two wavelengths that are differing by ($d\lambda_0$), with each producing a diffraction pattern at the focal plane, as shown in figure (3.18), will be displaced by ($d\lambda_0$) and given by equation (3.25).

$$d\lambda_0 = \frac{f_2 m}{d \cos(a)} d\lambda_0 \quad (3.25)$$

The closest the two wavelength patterns could be without merging into each other is given by the Rayleigh's criterion. As depicted in figure (3.18) the two wavelength patterns differing by (dl_0) could just be resolved if the maximum of one pattern coincides with the first minimum of the other. In this case $(dl_0 = Z_0)$. Substituting (Z_0) from equation (3.24) in equation (3.25) and from figure (3.18) using $(L\zeta = L\cos(a))$ gives the following expression for (dl_0) given by equation (3.26).

$$\boxed{\begin{aligned} dl_0 &= \frac{d}{Lm} l \\ &= \frac{Nm}{l} \\ &= \frac{R_0}{l} \end{aligned}} \quad (3.26)$$

where (N) is the total number of grooves in the grating.

The theoretical resolving power R is then given by equation (3.27).

$$R_0 = Nm \quad (3.27)$$

The values for the physical parameters of the optical components in MACS are given in equation (3.28) and table (3.1).

$m = 1.0$ $b = 0^{\circ}$ $N = 3.6 \times 10^4$ $f_1 = 31.0 \text{ cm}$ $f_2 = 16.0 \text{ cm}$ $d = 1.67 \times 10^{-3} \text{ mm}$ $d_f = 200.0 \text{ mm}$ $\text{pixel} = 24.0 \text{ mm}$ $R_0 = 3.6 \times 10^4$	(3.28)
--	--------

Table (3.1). A table showing the values for the angle of diffraction, the linear dispersion, the line width and the resolvable theoretical wavelength range for three different wavelengths using the physical parameters of the optical components used in MACS. In column 3 the reciprocal linear dispersion is calculated per pixel, which is the dimension of a pixel in the CCD camera used in MACS.

wavelength \AA	diffraction angle α degree	reciprocal linear dispersion $\frac{1}{LD} \text{\AA}/\text{pixel}$	spectral purity $d\lambda \text{\AA}$	resolvable theoretical wavelength range $d\lambda_0 \text{\AA}$
3600.0	12.47	2.44	10.77	10.00
4000.0	13.86	2.43	10.77	9.00
4500.0	15.63	2.41	10.77	8.00

The exposure time allowed to record the spectra is dependent on the source brightness, the light collecting area, the transmission efficiency of the telescope-spectrograph system, the slit dimension and the sensitivity of the detector. Consider a source of brightness given by equation (3.29).

$$f_1 \text{ Joules/sec/cm}^{-2}\text{/angs/steradians} \quad (3.29)$$

The flux received by the Schmidt-Cassegrain telescope is then given by equation (3.30).

$$f_1 = p_c \frac{\pi D_p^2 - D_s^2}{4} \text{ Joules/sec/angs/steradians} \quad (3.30)$$

where (D_p) and (D_s) are, respectively, the diameters of the primary and the secondary mirrors of the telescope.

The flux through a single fiber at the focal plane of the telescope is then given by equation (3.31).

$$f_1 = p_c \frac{\pi D_p^2 - D_s^2}{4} \frac{d_f}{F} \frac{d_f}{F} \text{ Joules/sec/angs} \quad (3.31)$$

In equation (3.31), (d_f / F) is the angle subtended by the height and width of a single fiber on the sky and F the effective focal length of the telescope.

Let (t_1) be the wavelength dependent transmission efficiency of the telescope-spectrometer combination.

The spectral flux received by a single pixel (E) is then given by equation (3.32).

$$E_1 = f_1 \cdot \frac{\pi D_p^2 - D_s^2}{4} \frac{\Delta \lambda}{\lambda} \frac{d_f}{F} \frac{d_f}{F} dl \frac{p^2}{wh} \cdot t_1 \text{ Joules/sec} \quad (3.32)$$

In equation (3.32) (w) and (h) are the projected fiber width and height on the detector and given by equations (3.10) and (3.11), respectively, (dl) the spectral purity and (p) the dimensions of a square pixel. From equation (3.32) the number photons of wavelength (λ) and energy ($h \cdot c / \lambda$) incident on a pixel per unit time (N_{photons}) is then given by equation (3.33) where (h_p) and (c) are the Planck constant and the speed of light, respectively.

$$N_{\text{photons}} = \frac{E_1}{h_p \cdot c / \lambda} \text{ sec}^{-1} \quad (3.33)$$

The basic detection mechanism of a CCD is related to the photoelectric effect where the light incident on the semiconductor produces electron-hole pairs. These electrons are then trapped in potential wells produced by numerous small electrodes. The maximum number of electrons that could be contained in each a pixel is called the well depth (**WD**). The quantum efficiency (**QE**) is the ratio of the actual number of photons detected to the number of photons incident at a given wavelength (λ). If the time taken

for a pixel to reach the well depth (**WD**) is (**T**) then the wavelength dependent integration time (**T**) is given by equation (3.34).

$$T = \frac{h \cdot c / l}{E_1 \cdot (QE)_1} \cdot (WD) \text{ seconds} \quad (3.34)$$

The physical parameters that are used in determining the integration time (**T**) are given in equation (3.35).

$D_p = 30.5 \text{ cm},$	$D_s = 10.2 \text{ cm}$	(3.35)
$d_f = 200.0 \text{ mm},$	$F = 192.0 \text{ cm}$	
$p = 24.0 \text{ mm},$	$f_1 = 31.0 \text{ cm}$	
$f_2 = 16.0 \text{ cm},$	$m = 1.0$	
$d = 1.67 \cdot 10^{-3} \text{ mm},$	$a = \sin^{-1} \frac{\lambda m l}{e d \theta}$	
$b = 0^\circ,$	$d l = 10.77 \text{ A}$	
$w = d_f \frac{\lambda f_2 \theta \cos(b)}{e f_1 \theta \cos(a)},$	$h = d_f \frac{\lambda f_2 \theta}{e f_1 \theta}$	
$c = 3.0 \cdot 10^8 \text{ ms}^{-1}$		
$h_p = 6.63 \cdot 10^{-34} \text{ Joules/sec}$		
$WD = 300,000$		
$QE(l = 3600 \text{ \AA}) = 0.32$		
$QE(l = 4000 \text{ \AA}) = 0.60$		
$QE(l = 4500 \text{ \AA}) = 0.70$		

The transmission efficiency (t_1) is a wavelength dependent parameter that depends on the transmission efficiency of the collimating lens, the fibers, the camera lens and the grating used in MACS and its wavelength dependent values are listed in table

(3.2). The number of optical surfaces that contribute to the transmission efficiency are listed in table (3.3). Table (3.4) gives effective transmission efficiency at different wavelength by considering the wavelength dependent transmission efficiencies given in table (3.2) and the number of optical surfaces through which the the light has to pass before entering the detector and given in table (3.3). Table (3.5) gives the K-coronal brightness at 1.1 and 1.6 solar radii at different wavelengths.

Table (3.2), The transmission efficiencies of the fibers, the lenses and the grating for three different wavelengths. This information is from figure (3.9), figure (3.11) and figure (3.12).

Wavelength Angstrom	Fibers	Lenses	Grating
3600.0	0.70	1.0	0.33
4000.0	0.90	0.99	0.32
4500.0	0.92	0.98	0.29

Table (3.3). The list of lenses and the associated number of surfaces through which the incident light had to pass before entering the detector.

Optical element	Number of surfaces
Corrector plate	2
Focal reducer	4
Collimating lens	4
Camera lens	4
CCD glass protector	2

Table (3.4) The effective transmission efficiency (t_1^{eff}) of MACS for the wavelengths 3600.0, 4000.0 and 4500.0 angstroms. The values are based on the information from tables (3.2) and (3.3).

Wavelength in angstrom	Effective transmission efficiency $t_1^{\text{eff}} = t_{\text{fiber}} \cdot t_{\text{lenses}}^{\text{NS}} \cdot t_{\text{grating}}$ (NS=number of surfaces)
3600.0	0.23
4000.0	0.25
4500.0	0.19

Table (3.5) The K-coronal brightness at 1.1 and 1.6 solar radii for three different wavelengths during the solar maximum. The values were obtained from Allen (1973) from pages 172 and 176. The units are in ergs/sec/cm²/angs/steradians. (1 Joule=10⁷ ergs)

Wavelength Angstrom	$f_1 \cdot 10^{-4}$ at 1.1 solar radii	$f_1 \cdot 10^{-4}$ at 1.6 solar radii
3600.0	6.21	4.26
4000.0	8.71	5.99
4500.0	12.33	8.47

Substituting equation (3.32) in equation (3.34) the expression for the integration time (T) is given by equation (3.36).

$$T = \frac{(h \cdot c / l) \cdot (WD)}{f_1 \cdot p \cdot \frac{e D_p^2 - D_s^2}{4} \cdot \frac{\theta}{F} \cdot \frac{d_f}{F} \cdot dl \cdot \frac{p^2}{wh} \cdot t_1^{eff} \cdot (QE)_1} \text{ seconds} \quad (3.36)$$

Using the values for the physical parameters from equation (3.35) and tables (3.4) and (3.5) gives the following chart, as shown in table (3.6), for the lower limit of the integration time (T) for the K-corona at 1.1 and 1.6 solar radii.

Table (3.6). Lower limit of the integration time for the K-coronal spectrum for MACS based on equation (3.36).

Wavelength angstrom	T in seconds at 1.1 solar radii	T in seconds at 1.6 solar radii
3600.0	122.0	177.0
4000.0	38.0	55.0
4500.0	27.0	39.0

However the actual integration time will depend on the amount of light absorbed by the various optical elements, the amount of light escaping the light collecting area of the optical elements and further contributions from the F-corona.

As for the spatial resolution of MACS the width of a single fiber of 200.0 μm and a plate scale of 0.107 arcseconds/ μm corresponds to a spatial scale of **21.4 μ** (0.022 solar radii). Taking the height of a single fiber as 200.0 μm and from equation (3.11) the projected height of the fiber on the spatial direction of the detector is given by equation (3.37).

$$\begin{aligned}
 h &= 200\mu\text{m} \cdot \frac{16.0 \text{ cm}}{31.0 \text{ cm}} \\
 &= 103.23\mu\text{m}
 \end{aligned}
 \tag{3.37}$$

This corresponds to (103.23 μm / 24.0 μm) 4.30 pixels in the spatial direction. Therefore from the spatial scale per fiber and the projected height of the fiber given in equation (3.37) the spatial resolution is given by equation (3.38).

$$\begin{aligned}
 \text{Spatial resolution} &= \frac{21.4\mu}{4.30 \text{ pixels}} \\
 &= 4.98\mu / \text{pixel} \\
 &\sim 5.19 \cdot 10^{-3} \text{ solar radii / pixel}
 \end{aligned}
 \tag{3.38}$$

3.4 Cost of the instrument

Table (3.7). Cost associated with the construction of MACS.

Item	\$ 000	Manufacturer
Telescope	6.79	Meade Corporation
Solar filters	1.02	Thousand Oak Optical
Fibers	4.05	Oriel Instruments
Collimating lens	1.39	Spindler & Hoyer
Camera lens	1.58	Spindler & Hoyer
Grating	2.35	American Holographic
CCD camera	10.5	Apogee Instruments
Camera software	0.60	PMIS
Computer	2.90	DPS 9000
GPS	0.41	Eagle Map Guide Pro
Glass base	0.45	United Glass Company
Spectrograph body	7.25	Lorr Company
Generator	0.77	Honda
Total	40.31	